

The climate change signal in the Mediterranean Sea in a regionally coupled atmosphere-ocean model

Ivan Parras-Berrocal¹, Ruben Vazquez¹, William Cabos², Dmitry Sein^{3,4}, Rafael Mañanes¹, Juan Perez-Sanz², Alfredo Izquierdo¹

- 5 ¹Applied Physics Department, University of Cadiz, Cadiz, 11510, Spain
²Department of Physics and Mathematics, University of Alcala, Alcala de Henares, 28801, Spain
³Alfred Wegener Institute for Polar and Marine Research, Bremerhaven, 27570, Germany
⁴[Shirshov Institute of Oceanology, Russian Academy of Science, Moscow, Russia](#)

10 *Correspondence to:* Ivan M. Parras-Berrocal (ivan.parras@uca.es)

Abstract. We assess the climate change signal in the Mediterranean Sea with the regionally coupled model REMO-OASIS-MPIOM (ROM). The ROM oceanic component is global with regionally high horizontal resolution in the Mediterranean Sea. In our setup the Atlantic and Black Sea circulations are simulated explicitly. Simulations forced by ERA-Interim show a good representation of the present Mediterranean climate. Our analysis of the RCP8.5 scenario driven by MPI-ESM shows
15 that the Mediterranean waters will be warmer and saltier across most of the basin by the end of the century. In the upper ocean layer temperature is projected to have a mean increase of 2.73°C, while the mean salinity increases by 0.17 psu, presenting a decreasing trend in the Western Mediterranean, opposite to the rest of the basin. The warming initially takes place at the surface and propagates gradually to the deeper layers.

Eliminado: role of ocean feedbacks in the simulation of the present climate and on the downscaled

1 Introduction

20 The Mediterranean Sea is expected to be among the world most prominent and vulnerable climate change “hot spots”. In this context, climate change lies at the heart of sustainable development in the Mediterranean. As such, the region is an optimal test bed for new approaches to science-society partnership sustained by the provision of adequate climate information and applicable to a broad range of vulnerable sectors. The Mediterranean is a regional sea circumscribed by Africa, Europe and Asia and divided into two sub-basins (eastern and western) through a sill that does not exceed 400 m depth between Sicily
25 and the African continent. The freshwater balance in the Mediterranean basin is negative, since the evaporation exceeds rainfall and river run-off (Sanchez-Gomez et al., 2011). This deficit is compensated by a net inflow of water through the Strait of Gibraltar. The region is located in a transitional area between tropical and mid-latitudes and presents a complex orography and coastlines where intense local air-sea and land-sea interactions take place. These intense local air-sea interactions together with the inflow of Atlantic water drive the Mediterranean thermohaline circulation (MTHC) (Fig. 1).
30 For these reasons, atmosphere-ocean regional coupled models (AORCMs) are essential for the study of atmospheric and oceanic processes in the Mediterranean Sea.

Eliminado: The region is located in a transitional area between tropical and mid-latitudes and presents a complex orography and coastlines where intense local air-sea and land-sea interactions take place. The freshwater balance in the Mediterranean basin is negative,

To date, different AORCMs with typical horizontal resolution of 25-50 km in the atmosphere and 10-20 km in the ocean have been developed to study the climate of the Mediterranean Sea (Somot et al., 2008; L'Hévéder et al., 2013; Sevault et al., 2014; Cavicchia et al., 2015; Darmaraki et al., 2019). However, Akhtar et al. (2018) found the higher horizontal resolution (9 km) in the atmosphere improves the simulation of the wind and the turbulent heat fluxes, although they conclude that a higher resolution models do not perform better in all aspects than coarser configurations. Somot et al. (2008) developed the Sea Atmosphere Mediterranean Model (SAMM), which meant a new concept of AORCMs, composed by the coupling of the atmospheric global model (ARPEGE) (Déqué and Piedelievre, 1995) and the regional high-resolution (10 km) ocean model (OPAMED; Somot et al., 2006). Their results under the A2 (IPCC, 2000) climate change scenario showed an increment at the end of the 21st century of temperature and salinity both in shallow (3.1°C and 0.48 psu) and in deeper layers (1.5°C and 0.23 psu) of the Mediterranean Sea (Somot et al., 2006). In 2013 the European CIRCE project was launched (Gualdi et al., 2013), in order to ease the coordination among the scientific community responsible for regional climate modeling in the Mediterranean. The beginnings of CIRCE was can be traced to the work of Dubois et al. (2012) who compared different AORCMs and regional climate models (RCMs). In addition, these authors analyzed a projection (1950-2050) of the Mediterranean climate under the A1B scenario simulated by an ensemble of five coupled regional models. For the first time, atmosphere-ocean realistic net flows were obtained that predict a Mediterranean surface warming between +0.8°C and +2°C. Shaltout and Omstedt (2014) analyzed the Mediterranean SST for the 2005-2100 period projected by ensembles of CMIP5 (Taylor et al., 2012) global models under the RCP2.6, RCP4.5, RCP6.0 and RCP8.5 scenarios. The CMIP5 ensembles means indicate a warming, which ranges from +0.5°C in the RCP2.6, through +1.15°C in the RCP4.5, +1.42°C in the RCP6.0, to +2.6°C in RCP8.5 scenario. The authors conclude that the warming is mainly controlled by the amount of greenhouse gas emissions. More recently, Adloff et al. (2015) found that the mean Mediterranean SST and SSS will increase between +1.73 and +2.97°C, and +0.48 and +0.89 psu at the end of the 21st century. Their results were based on an ensemble of six simulations performed with different configurations of the NEMOMED8 (Beuviel et al., 2010) ocean model under different scenarios. Darmaraki et al. (2019) employed an ensemble of 17 fully coupled atmosphere-ocean simulations to study the evolution of SST and marine heat waves in the Mediterranean Sea for 1976-2100 period. The ensemble means by the end of the century indicates a +3.1°C increase of Mediterranean mean SST under the RCP8.5 scenario. By 2100, as a response of the sea surface warming, projections showed stronger and more intense Mediterranean marine heat waves. Most of these authors agree that the choice of emission scenario is the most important conditioning for the expected warming of the Mediterranean Sea.

These modeling efforts are coordinated through the Med-CORDEX initiative (Ruti et al., 2015; www.medcordex.eu), which is the regional climate modelling taskforce of the HyMeX program (www.hymex.org). In these models the oceanic component of the RAOCMs is also regional. The use of an oceanic global model (MPI-OM) in REMO-OASIS-MPIOM (ROM) coupled system model, could help to avoid some problems associated with the open boundary conditions for the Mediterranean Sea, allowing to study processes that take place in the Mediterranean region but which have its origin at the North Atlantic Ocean. This work aims to contribute to the Med-CORDEX initiative with a first detailed evaluation of high-

Eliminado: Artale et al., (2010) used the PROTHEUS model driven by ERA-40 reanalysis, to reproduce present climate of the Mediterranean Sea. PROTHEUS use the Mediterranean regional configuration of MITgcm (Sannino et al., 2009) ocean model coupled to RegCM3 atmospheric model (National Center for Atmospheric Research, NCAR). More recently L'Hévéder et al., (2013) designed the LMDz-NEMO-Med model implemented by the coupling of the regional atmospheric model LMDz4 (Hourdin et al., 2006) and NEMOMED (Beuviel et al., 2010) ocean model, forced by ERA-40 reanalysis. Dell'Aquila et al., (2012) were the first authors to add the river coupling to RAOCMs through the spatial integration of the simulated monthly total runoff (TRIP dataset; Oki and Sud, 1998) over a large portion of the Mediterranean basin.

Eliminado: Finally, Sevault et al., (2014) developed a fully coupled regional climate system model (CNRM-RCSM4) dedicated to the Mediterranean region and performed a multidecadal hindcast simulation (1980-2012) driven by global atmosphere and ocean reanalysis. CNRM-RCSM4 includes the regional representation of the atmosphere (ALADIN-Climate model; Herrmann et al., 2011), land surface (ISBA model; Noilhan and Mahfouf, 1996), rivers (TRIP model; Oki and Sud, 1998), and the ocean (NEMOMED 8 model; Beuviel et al., 2010) with a daily coupling through the OASIS coupler (Valcke, 2013).

resolution atmosphere-ocean simulations with the coupled ROM model, which has been used for some previous multimodel studies (see e.g. Darmaraki et al., 2019). Here we analyze the evolution of Mediterranean Sea under the RCP8.5 scenario with boundary conditions taken from CMIP5 simulation with the MPI-ESM global model. Especially, we focus on water masses properties such as SST and SSS and their evolution at the end of 21st century.

5 The objectives of this study can be summarized as follows:

- (i) Assess the skills of ROM in reproducing the observed regional climate over the Mediterranean Sea when driven by ERA-Interim reanalysis.
- (ii) Examine the added value that high-resolution ROM brings with respect to the driving global model in the area of study, when forced by MPI-ESM.
- 10 (iii) Assess the projected climate change signal in the Mediterranean Sea in the RCP8.5 scenario.

This paper is organized in the following way: a general description of our coupled model and each of its components is given in section 2. In section 3, we present the results of the validation followed by the coupled model simulations for the Mediterranean region. Finally, section 4 contains the discussion and 5 the conclusions.

2 Methods

15 For this work, the ROM climate model has been used (Sein et al., 2015). ROM comprises the REgional atmosphere MODEL (REMO; Jacob et al., 2001), the Max Planck Institute Ocean Model (MPI-OM; Marsland et al., 2003; Jungclaus et al., 2013), the HAMBurg Ocean Carbon Cycle (HAMOCC) model (Maier-Reimer et al., 2005), the Hydrological Discharge (HD) model (Hagemann and Gates, 1998, 2001), the soil model of REMO (Rechid and Jacob, 2006) and a dynamic/thermodynamic sea ice model (Hibler, 1979) which are coupled via OASIS3.0 (Valcke, 2013) coupler, and was
20 called ROM by the initials REMO-OASIS-MPIOM.

2.1 Atmosphere (REMO)

The atmospheric component of ROM is the REMO. The dynamic core of the model and the discretization in space and time are based on the Europa-Model of the Germany Weather service (Majewski, 1991). The physical parameterizations are taken from the global climate model ECHAM versions 4 and 5 (Roeckner et al., 1996, 2003). The variables which exchange info
25 between REMO and MPI-OM via OASIS are 10 m wind velocity, wind stress over water, wind stress over sea ice, liquid precipitation, solid precipitation, net shortwave radiation, total heat flux over water, conductive heat flux and residual heat flux (Fig. 2a). To avoid the largely different extensions of the grid cells close to the poles, REMO uses a rotated grid, with the equator of the rotated system in the middle of the model domain. The horizontal discretization is done on the Arakawa C-grid and the hybrid vertical coordinates are defined according to Simmons and Burridge (1981). More information about the
30 parameterizations of atmospheric component can be found in Sein et al. (2015).

2.2 Ocean (MPI-OM)

The oceanic component of ROM is the MPI-OM developed at the Max Planck Institute for Meteorology (Hamburg, Germany). MPI-OM is a free surface, primitive equations ocean model, which uses the Boussinesq and incompressibility approximations. MPI-OM is formulated on an orthogonal curvilinear Arakawa C-grid (Arakawa and Lamb, 1977) with variable spatial resolution. This grid allows for the placement of the poles over land, thus removing the numerical singularity associated with the convergence of meridians at the geographical North Pole. An additional advantage of the curvilinear grids is that a higher resolution in the region of interest can be reached, while maintaining a global domain. Using the global ocean model alleviates issues related to ocean open boundary conditions and provides an additional “degree of freedom” in the model setup and tuning, which can be helpful to adjust the ocean component for the better performance within the region of interest. The model parameterizations and setup are detailed in Sein et al. (2015).

2.3 ROM experiment set-up

Fig. 2a shows the coupling scheme used in ROM. In the region covered by REMO the atmosphere and the ocean interact while the rest of the global ocean is driven by energy fluxes, momentum and mass from global atmospheric data used as external forcing. In the experiments analyzed here, data from ERA-Interim reanalysis (Dee et al., 2011) and MPI-ESM (Giorgetta et al., 2013) are used to provide lateral boundary conditions to REMO and to force MPI-OM outside the coupling region.

The MPI-OM grid used in this setup is represented by black lines in Fig. 2b. In the Mediterranean region the highest horizontal resolution of MPI-OM is 7 km (south of the Alboran Sea) while the lowest resolution is 25 km (eastern coasts of Mediterranean Sea). In the vertical MPI-OM has 40 z-levels with increasing layer thickness with depth. The REMO domain covers the North and Tropical Atlantic, a large part of Africa, South America and Mediterranean region (red line, Fig. 2b) with a resolution of about 25 km on a rotated grid. [More information about the ROM coupled system is summarised in Table 1.](#) The HD model (global domain) computes the river discharge at 0.5° resolution. The atmosphere and ocean exchange information [each 60 minutes](#), while HD interacts with MPI-OM and REMO each 24 hours (Fig. 2a).

[In this work, 30-year time series from three different experiments have been analyzed. The first simulation, thereafter ROM_P0, was forced by ERA-Interim for 1980-2012 and used to assess the skills of ROM in reproducing the observed regional climate over the Mediterranean Sea. In order to offer an integrated vision of the impact introduced by the climate change in the Mediterranean Sea, we make a dynamical downscaled of present time simulation with MPI-ESM-LR which covers 1950-2005 period \(for our analysis we take from 1976-2005, ROM_P1\) and a climate change projection from 2006-2099 \(for our analysis we take from 2070-2099, ROM_P2\) under the Representative Concentration Pathways 8.5 \(RCP8.5\) scenario.](#)

2.4 Validation Methodology

The ROM present Mediterranean climate is analyzed in terms of mean state, seasonal cycle and interannual variability of the main atmospheric and oceanic variables. For the ROM atmospheric component REMO, three representative variables were chosen: Mean Sea Level Pressure (MSLP), near-surface temperature (T2m) and precipitation; while for the ocean component MPI-OM: Sea Surface Temperature (SST), Sea Surface Salinity (SSS), Sea Surface Height (SSH) and the velocity components of the sub-surface current. These fields are compared to gridded data from different sources to evaluate the ability of ROM model to simulate the present Mediterranean climate. These data sets are derived from observations or reanalysis where appropriate (Table 2).

For MSLP and T2m we compare the output of ROM with ERA-Interim reanalysis. The ERA-Interim data assimilation system uses a 2006 release of the Integrated Forecasting System (IFS) developed jointly by ECMWF and Météo-France. The spatial resolution of data set is approximately 80 km (T255 spectral) on 60 vertical levels from the surface up to 0.1 hPa (Dee et al., 2011); free access data can be found at <https://www.ecmwf.int/en/research/climate-reanalysis/era-interim>. Total precipitation was validated against the Tropical Rainfall Measuring Mission (TRMM; Huffman et al., 2014) dataset, a joint mission between NASA and the Japan Aerospace Exploration Agency (JAXA) to study rainfall for weather and climate research.

Three datasets were used for the evaluation of the SST: ERA-Interim, EN4 and OISST. For the development of EN4 data set Good et al. (2013) performed a 1-degree monthly objective analysis from ocean temperature and salinity bathythermograph profiles (MBT, XBT). The version EN4.1.1 used here includes the improvements on the estimation of MBTs and XBTs downward velocity developed by Gouretski and Reseghetti (2010). On the other side, the NOAA performed an analysis constructed by combining observation from different platforms (satellites, ships, buoys) on a regular global grid $1/4^\circ \times 1/4^\circ$, known as Optimum Interpolation Sea Surface Temperature (OISST; Reynolds et al., 2007). Currently, the OISST dataset is considered the best-observed SST dataset available, in terms of spatial and temporal resolution.

To validate ROM SSS, we made comparisons with two climatologies: EN4 v.4.1.1 (Good et al., 2013) and MEDSEA_REANALYSIS_PHY_006_009 (Fратиanni et al., 2015) implemented by Copernicus Marine Environment Monitoring Service (CMEMS). MEDSEA_REANALYSIS_PHY_006_009 is based on the NEMO code, the data assimilation scheme is variational, and all historical (1955-2015) in-situ and satellite observations were used. The model is primitive equation in spherical coordinates implemented for the Mediterranean at $1/16^\circ \times 1/16^\circ$ horizontal resolution (Fратиanni et al., 2015).

For a better assessment of ROM's potential to improve the simulation of the climate in the Mediterranean Sea comparisons against Earth Systems Models (ESMs) are required. The MPI-OM local high-resolution ocean setup employed in the ROM configuration is different from the global MPI-OM used in Max Planck Institute-Earth System Model (MPI-ESM). MPI-ESM (Giorgetta et al., 2013) is composed by ECHAM 6 (Stevens et al., 2013) for atmosphere and MPI-OM (Jungclaus et al. 2013) for ocean as well as JSBACH (Reick et al., 2013) for terrestrial biosphere and HAMOCC (Ilyina et al., 2013) for the

ocean's biogeochemistry. The coupling of the atmosphere, ocean and land surface is made possible by the OASIS3 (Valcke, 2013) coupler. Depending on the resolution of the ECHAM6 or MPI-OM the MPI-ESM has different configurations (MPI-ESM-LR (low resolution), -MR (medium resolution); the -LR uses a bipolar grid with 1.5° resolution, while the -MR version doubles the number of levels in the atmosphere and decreases the horizontal grid spacing of the ocean to 0.4° (Giorgetta et al., 2013).

3 Results

In this section, a selection of key fields corresponding to the period 1980-2012 ([ROM_P0](#)) is presented. In a second step changes in the Mediterranean Sea state under RCP8.5 conditions are estimated from the analysis of differences between present climate (1976-2005, [ROM_P1](#)) and the climate projection (2070-2099, [ROM_P2](#)).

3.1 Atmosphere validation

Mean sea level pressure (MSLP) is a good indicator of large-scale circulation, which influences near-surface temperature (T2m) and precipitation distributions. Erroneous MSLP gradients lead to an erroneous regional wind circulation, and can also have a strong effect on ocean circulation (Sein et al., 2015). Figs. 3a and 3b display the biases of modeled MSLP with respect to ERA-Interim for the boreal winter (defined as December, January, and February; DJF) and summer (defined as June, July, and August; JJA) in the 1980-2012 period ([ROM_P0](#)).

According to Figs. 3a and 3b ROM provides a good agreement with ERA-Interim MSLP, showing maximum deviations smaller than 3 hPa over most of the domain for both seasons. The strongest departures can be found in DJF, due to an overestimation of the Azores high during the winter months. Those differences could be attributed [partly](#) to REMO parameterizations, [but a more important role could be played by the deficiencies in the simulated ocean circulation in the North Atlantic, which are analyzed in a paper in preparation](#). Nonetheless, these relatively small deviations imply a small change in terms of regional wind circulation. During summer months (Fig. 3b) MSLP biases are much smaller over the Mediterranean.

Figs. 3c and 3d show T2m biases for DJF and JJA. For both seasons the departures are typically below 3°C over most of the coupled domain, except for the Alps, the Pyrenees, the Atlas, the Caucasus and the Armenian highlands (Figs. 3c and 3d).

This disagreement can be attributed to differences in the resolution of orographic features. Winter months show the largest T2m biases located close to the Mediterranean coastline, where atmospheric-ocean interactions could play a role.

At first glance, ROM generally underestimates the simulated cumulative precipitation over most of the Mediterranean region, for both winter and summer seasons. The largest discrepancies for DJF can be located over the Black Sea, the Adriatic Sea, the Gulf of Lions and the southwest portion of Iberian Peninsula (Fig. 3e), where negative anomalies can reach

3mm/d. Moreover, it is worth stating that during the same period the total precipitation was overestimated in regions linked to significant topographic reliefs (e.g. the Alps). Some coastal areas also showed positives anomalies that probably are

related to the atmosphere-ocean coupling. In the very dry summer season, ROM shows a clear tendency to underestimate the precipitation (Fig. 3f). Over the ocean, this bias can be related to the cold SST bias, common to the most of the AORCMs simulations of the Mediterranean climate (see Darmaraki et al., 2019). The seasonal mean precipitation is reasonably well simulated by our coupled system along the most of the Mediterranean basin. However, the ROM simulation shows significant systematic errors (up to ± 3.5 mm/d) remain substantial over the region in terms of precipitation.

The impact of interactive atmosphere-ocean coupling in REMO is shown in Fig. 4, presenting the climatology differences between ROM and stand-alone REMO in the simulations forced by ERA-Interim for MSLP, T2m, and precipitation. Over land the simulated fields have a larger dependency on the internal details of the atmospheric component, and the impact of the coupling is dependent on the large-scale circulation and land-sea contrasts. Therefore, we can expect the differences over land to be overly small, except for the regions where the large-scale circulation or the land-sea contrasts are important. The winter MSLP over the Atlantic is higher in the coupled run (Fig. 4a), causing an anomalous strong anticyclonic circulation that extends to land and the Mediterranean Sea, west of the Balearic Islands. The large-scale influence of the Atlantic anomalous circulation offsets the effect of the warmer SST here (see Fig. 5, where the SST biases are represented). However, elsewhere over the Mediterranean Sea, where the ROM SST is colder (warmer) than ERA-Interim, a higher (lower) MSLP is simulated by ROM. In summer (Fig. 4b), the differences in MSLP seem to be determined mainly by the colder SST in ROM, which leads to higher MSLP in the model than in the reanalysis.

The changes in T2m induced by the coupling over the Mediterranean (Figs. 4c and 4d) seem to be mainly determinate by the SST, through the turbulent heat fluxes. In both seasons the T2m differences induced by the coupling correspond very well with the SST biases with respect to ERA-Interim. However, in winter T2m seems to be also influenced by the transport of Atlantic air carried by the anomalous anticyclonic circulation simulated in the Atlantic. Over land the differences in winter T2m are mainly determined by the changes induced in large scale circulation by the interactive SST in the Atlantic, while in summer the land-sea contrasts seem to be more important.

The differences between the SST from ERA-Interim and the simulated by ROM is also reflected in the rainfall simulated by REMO and ROM (Figs. 4e and 4f). In winter the Mediterranean Sea regions where the ROM SST is warmer have a higher precipitation, while colder ROM SST leads to a lower precipitation. The impact of the SST biases on the precipitation is clearer in summer: the cold SST bias leads in ROM to a precipitation which is weaker than in the REMO simulation all over the Mediterranean Sea, especially in the northern part, where the reduction of precipitation in ROM with respect to REMO is comparable in magnitude to the ROM precipitation bias (Fig. 3f).

Eliminado: these deviations did not exceed 3.5 mm/d allowing us to assume that our regional coupled model reasonably simulates the precipitation along the Mediterranean basin. By contrast, these deviations are minimal in the very dry summer season, although ROM shows a clear tendency to underestimate the precipitation (Fig. 3f).

3.2. SST

30 3.2.1 Seasonal cycle

The differences between ROM and observed SST climatologies for winter (DJF) and summer (JJA) in the 1980-2012 period are presented in Fig. 5. The SST seasonal cycle is well represented by the model, although its amplitude is reduced over most

of the Mediterranean Sea. The deviations in absolute value do not exceed 3°C, although ROM shows a cold bias, which is more significant in the eastern Mediterranean, especially in summer (Fig. 5).

In DJF ROM overestimates SST over the Mediterranean northern coasts and the whole western basin, showing positive biases reaching 2°C (Figs. 5a, 5b and 5c). In summer, the negative SST extends over a large part of the Mediterranean domain (Figs. 5d, 5e, and 5f) indicating that the model is simulating colder temperatures than expected for JJA.

In order to assess the improvement that higher resolution in ROM brings to the simulation of the present Mediterranean climate, comparisons with MPI-ESM-LR and -MR have been done (Fig. 6):

SST seasonal cycle amplitude is smaller in ROM than in MPI-ESMs, with warmer DJF and colder JJA. The SST bias is between ±3°C in the whole Mediterranean basin. In winter, ROM shows warmer temperatures than MPI-ESM (-LR and -MR, Figs. 6a and 6b) with the exception of southeastern Mediterranean coasts where negative differences appear (near to -1°C). In JJA a cold bias is presented into the western basin (-1.5°C), southern coasts (-0.5°C), Levantine and Aegean seas (-3°C) while into the Tyrrhenian, Adriatic and Ionian seas low positive anomalies (up to +1°C) are presented (Figs. 6c and 6d).

Eliminado: overestimates the SST simulated by MPI-ESM (-LR and -MR, Figs. 5a and 5b)

3.2.2 Interannual variability

Fig. 7 shows a time series of yearly mean SST averaged over the Mediterranean Sea for the 1980-2012 period. The ROM yearly mean SST shows cold biases (from 0.1 to 1.4°C) against ERA-Interim, EN4 and OISST datasets. Compared to ERA-Interim (purple line) this cold bias increases from 0.6°C in 1980 to 0.8°C in 2012, while the averaged cold bias is -0.6°C compared to OISST (red line) for the full period. The largest deviations are found for EN4 (yellow line) due to dataset configuration.

The increasing trend of modeled SST is weaker than in the observed climatologies (Table 3) due to the absence of effects introduced by aerosols. Despite these small differences, the interannual variability and the trend is well reproduced by ROM simulation during 1980-2012 period. An offset of SST is visible in Fig. 7, although it keeps constant during all period.

A Taylor diagram (Fig. 8) was used to quantitatively evaluate ROM performance. ERA-Interim, EN4 and ROM are all well correlated ($r > 0.7$) with the observation-based climatology (OISST). However, the SST standard deviation of ROM (0.27°C) is lower than OISST (0.32°C), while ERA-Interim, EN4 present closer values (0.34 and 0.33°C, respectively). The corresponding root-mean-square-errors (RMSE, red contours) are enclosed by 0.07 and 0.22°C, being ROM close to the climatological uncertainty.

Eliminado: Although the MPI-ESM and ROM results looks qualitatively similar, ROM better captures the peaks of interannual variability than both -LR and -MR MPI-ESM simulations.

Eliminado: MPI-ESM-LR and -MR correlations with OISST are lower. T...

Eliminado: and MPI-ESM-LR

Eliminado: In general ROM improves the scores obtained by MPI-ESM simulations, since ROM shows higher correlation and lower RMSE with respect to OISST.

Eliminado: 2.2

3.3 SSS

Fig. 9 shows the differences between the SSS modeled by ROM and the selected reanalysis averaged for DJF and JJA during 1980-2012. In all comparisons a common pattern in spatial SSS bias distribution is observed, showing positive bias over the western basin and Adriatic Sea and negative bias through the Levantine Sea and north Aegean Sea. It is precisely at northeast Adriatic Sea, by the Po Delta, where the largest positive differences occur (+3 psu), and to the north of the Aegean

Sea where largest negative differences (-3 psu) are found. Nevertheless, the deviations do not exceed, in absolute value, 0.5 psu in a large part of the domain (Fig. 9).

Comparison with MPI-ESM-LR and -MR SSS is shown in Fig. 10. ROM is always saltier over the whole Mediterranean, with decreasing difference towards the southeast. In general, ROM SSS is closer to EN4 and CMEMS climatology than any of the MPI-ESM versions.

3.4 SSH and circulation

To conclude with the analysis of the ocean component of ROM, the SSH was analyzed. The time-averaged SSH and horizontal current velocity at 31 m depth simulated by ROM between 1980-2012 are shown in Fig. 11. It is clearly seen how Atlantic surface waters enter through the Strait of Gibraltar to the Western Mediterranean; after crossing the Alboran Sea the inflow jet run near to the African continent coastline. At the Strait of Sicily, part of the Atlantic water moves northward along the coast of the Tyrrhenian Sea, while the rest continues flowing to the Eastern basin. ROM reproduces quite clearly the places where deep water formation takes place, especially in the Gulf of Lions, southern Adriatic Sea and in the Levantine Sea (near Crete and Rhodes islands) with the presence of three cyclonic gyres. These cyclonic gyres concur with negative SSH values, which highlights the sinking of surface waters. The mean SSH closely reproduce the well-established steady basin and sub-basin scale circulation pattern (e.g. Bergamasco and Malanotte-Rizzoli, 2010). However, some of the meso-scale structures of circulation may escape the model horizontal resolution in the Eastern basin (ca. 25 km).

A first approximation for properly comparing the SSH of the model to the AVISO Sea Level Anomaly (SLA) (SSALTO/DUACS, 2013) is to add only the thermosteric contribution (as a constant resulting from the average over the whole basin) to the dynamic SSH of the model (Sevault et al., 2014). Fig. 12 shows the yearly mean and the seasonal cycle of ROM SSH compared to altimetric data. The modeled SSH shows lower values than the observed (Fig. 12a); however, it represents quite acceptably the behavior of AVISO time series. The amplitude of the mean seasonal cycle is 12 cm for the simulation, and 14.5 cm for AVISO (Fig. 12b). Thus, the model is able to reproduce a realistic interannual variability and seasonal cycle.

Finally, a mass balance was made to estimate the net transport of water throughout the Strait of Gibraltar and Dardanelles in order to compare the water flux modeled by ROM with the observations. Table 4 gives the water budget of ROM averaged over the 1980-2012 period. The water loss by evaporation (E) is greater than the gain by precipitation (P) and river runoff (R) generating a deficit of 0.034 Sv into the basin. However, this deficit is partially compensated by the net water inflow through the Strait of Gibraltar (0.03 Sv) and the Dardanelles, where the inflow (0.132 Sv) exceeds the outflow (0.109 Sv). ROM water budget is 0.026 Sv lower compared to RCSI4 model, but a significant part of the difference is due to difference in river runoff.

Eliminado: 2.3

3.5 Projections under RCP8.5 scenario

Projections performed by the ensembles of ESMs collected by the IPCC (2013) under the conditions of different scenarios anticipate that the climate change will cause a generalized and perceptible global warming of the oceans, at surface and deeper layers at the end of 21st century.

5 Fig. 13 shows the mean SST and SSS fields for the present climate (1976-2005, ROM P1) together with the differences with respect to future projections under the RCP8.5 scenario (ROM P2-ROM P1). The averaged zonal SST gradient over most of the Mediterranean Sea increases from north to south. The western Mediterranean is colder than the eastern, especially in the Gulf of Lions and in the northern Adriatic Sea where the SST minima are located (Fig. 13a). The warmest area is found along the Levantine Sea coastline. The averaged Mediterranean SST is 18.61°C (Fig. 13a) while at the end of the 21st century under RCP8.5 scenario it is expected to have a mean increase of +2.73°C, warming in a range from a maximum of 3.8°C at the Aegean Sea to a minimum of 0.9°C at the Alboran Sea (Fig. 13b).

To verify that the trend remains stable and it is not affected by a strong ROM's SST bias, comparisons for DJF and JJA have been performed separately (see Supplementary Figures). Noting the results, the trend analysis is not affected by the SST bias (Fig. 5).

15 As shown in Fig. 13c the Eastern Mediterranean is saltier than western, particularly in the Levantine Sea (39 psu). The Western basin presents lower salinities (< 38.25 psu) influenced by the inflow of Atlantic freshwater through the Strait of Gibraltar (36.6 psu) along the African coasts up to the Ionian Sea. Another source of freshwater is located at the Dardanelles strait where the water from the Black Sea has salinities lower than 35 psu. The averaged Mediterranean SSS is 38.02 psu while under the RCP8.5 projection it will experience a mean increase of 0.17 psu. The differences between the mean SSS projection and present climate shows a dipolar structure through the Mediterranean Sea (Fig. 13d). Under the RCP8.5 scenario, the Western Mediterranean is expected to slightly freshen (from -0.5 to -1 psu), while the Eastern will become saltier. It is precisely at the north of the Aegean Sea where largest SSS increases (+4 psu) are found.

20 In general, MPI-ESM-LR and -MR projections under the RCP8.5 scenario at the end of the 21st century are warmer than that of ROM over most of the Mediterranean Sea. Namely, the projected mean SST increases are 2.80 and 2.87°C for MPI-ESM-LR and -MR, respectively (Table 5). Despite differences in horizontal resolution, MPI-ESM-LR and ROM show a similar spatial distribution of the expected warming (Fig. 14a), contrary to MPI-ESM-MR where the SST warming is projected to be higher in the western basin and north of Adriatic Sea (Fig. 14b).

25 ROM projection is always saltier at surface than any MPI-ESM version over the whole Mediterranean basin. The mean SSS change for the 2070-2099 period with respect to 1976-2005 in MPI-ESMs shows the same spatial pattern than ROM model (Figs 14c and 14d). The MPI-ESM-LR forced by the RCP8.5 scenario shows a SSS mean increase of 0.10 psu while for the -MR of 0.12 psu.

30 Fig. 15 shows the mean temporal evolution of temperature and salinity anomalies in the water column over the Western and Eastern Mediterranean along the 21st century according to ROM projection for the RCP8.5 scenario. To calculate these

anomalies in a given region we first average horizontally, as indicated in Fig. 15 insets, the temperature and salinity in each model level for the present time period (1976-2005) and the RCP8.5 projection period (2006-2099). The anomalies are defined as the difference between the time series for RCP8.5 scenario (2006-2099) and the time mean for the present climate period (ROM_P1). The Mediterranean Sea shows an increase of its temperature through the entire water column (Figs. 15a and 15c), which is more evident in surface layers. The warming that initially takes place in the upper ocean propagates gradually to deeper layers along the 21st century. The behavior of the Eastern Mediterranean is similar to that of the western basin, but with warmer temperatures, especially in the surface layers. At the end of the 21st century the eastern basin is expected to have a surface temperature increase up to 3.8°C (Fig. 15a) and the western up to 3°C (Fig. 15c). In deeper layers (1000 m) the water temperature will increase by 0.6°C for both basins, which is a very significant warming at these depths.

The mean temporal evolution of salinity anomalies displays different patterns through the Mediterranean Sea. During the 21st century the upper layer (0-100 m) of the Western Mediterranean is projected to freshen (-0.5 psu) while the deeper layers tends to get saltier up to 0.5 psu. However, the Eastern Mediterranean will increase its salinity up to 0.5 psu in the entire water column along the current century.

4 Discussion

AORCMs are capable of improving the simulation of the climate system by the driving model through dynamical downscaling from GCMs (e.g. Li et al., 2012; Sein et al., 2015). The regionalization implemented in our ROM model provides higher horizontal resolution, allowing the representation of local scale and mesoscale processes that are not detectable by MPI-ESM. For instance, the exchange through the Gibraltar and Dardanelles Straits are well resolved in ROM. Also, ROM is able to give a good representation of the main characteristics of the ocean circulation in the Adriatic Sea, while in MPI-ESM-LR the ocean model is not able to represent these features due to the lack of the necessary horizontal resolution. Compared to other state-of-art regional climate models, ROM introduces a remarkable innovation, which consist in the implementation of a global oceanic model with high horizontal resolution at regional scales. This approach allows to obtain information of the global ocean without losing spatial resolution in the coupling area. An important disadvantage of the proposed model, related previously in Sein et al. (2014), is that the bias and internal variability generated from the global domain can influence the results in the coupled domain, making it difficult to separate the source of bias.

ROM shows good skills in reproducing the main characteristics of the climate of the Mediterranean Sea. The biases of the main atmospheric and oceanic parameters are in the range shown by other state of art regional models (L'Hévéder et al., 2013; Sevault et al., 2014; Akhtar et al., 2018; Darmaraki et al., 2019).

The seasonal MSLP was validated against ERA-Interim, showing biases smaller than ± 3 hPa over most the domain for DJF and JJA, a performance similar to other models (see e.g. Giorgi and Lionello, 2008). Positive MSLP biases over a large extend of the domain during DJF (Fig. 3a) could generate anticyclonic conditions which lead a greater stability and lower storm generation; while in JJA (Fig. 3b) the biases are generally much lower. With respect to the seasonal cycle of near-

surface atmospheric parameters such as near-surface (2m) temperature (T2m) and precipitations, the LMDz-NEMO-Med coupled model (L'Hévéder et al., 2013) gives a bias range of (-4; +4°C/-2; +3 mm/d, respectively) which is comparable to the ROM estimates (Figs. 3c, 3d, 3e and 3f). Similarly, to most of Mediterranean regional models, ROM shows a higher than observed rainfall over areas with pronounced topography such as the Alps (Artale et al., 2010; L'Hévéder et al., 2013; Di Luca et al., 2014). More recently, Fantini et al. (2016) also reported a similar bias (± 3 mm/d) in an ensemble of regional coupled models forced by ERA-Interim. Panthou et al. (2018) observed that for heavy precipitation increasing resolution increases the wet biases. We totally agree with the final consideration of Fantini et al. (2016), which proposed that to improve the performance RCMs simulating precipitation it is necessary the availability of high quality and high-resolution observation for the assessment of the models.

The comparison of the ROM with standalone REMO shows that the changes in SST generated by the coupling in the Atlantic Ocean influence the simulated Mediterranean climate, causing a spurious anticyclonic circulation in winter which impacts the surface temperature in the Western Mediterranean. In summer the modeled SST is significantly colder than observations, leading to colder T2m and less precipitation over the basin, as the colder SST reduces the evaporation. Regarding the oceanic parameters, ROM shows biases within $\pm 3^\circ\text{C}$, correlation coefficients above 0.7 and RMSE below 0.25°C when compared to ERA-Interim, EN4 and OISST data sets. ROM presents cold biases along the Eastern Mediterranean that become stronger and extend to the whole basin in summer months. The summer biases are common to most of the Mediterranean regional coupled simulations (see for instance, Dubois et al., 2012; Li et al., 2012, Sevault et al., 2014). Akhtar et al. (2018) studied the impact of resolution and coupling in modelling the climate of the Mediterranean Sea and concluded that coupling generates a negative bias in SST. Most recently, Darmaraki et al. (2019) assessed an ensemble of 17 simulations from six models, in which our ROM coupled system was included. Their results showed an averaged cold bias ranging from (-0.29 to -1.01°C) when regional models are compared to satellite data. When forced by ERA-Interim, ROM shows averaged Mediterranean SSTs that are colder than reference climatologies during 1980-2012 period (Fig. 7), a common trait with other RCMs (Sevault et al., 2014; Ruti et al., 2015). Macias et al. (2018) showed that a simple spatially-uniform bias correction improves the simulated surface oceanic conditions of the Mediterranean basin when forcing an oceanic model with atmospheric data from RCM realizations. These results show the summer biases could be related either to a deficit of solar radiation by the atmospheric model or to shortcomings in the simulation of some processes in the ocean model, as vertical mixing or turbidity. As these biases appear in the coupled runs, we could speculate that some coupling feedbacks are present. This topic deserves a separated study and will be tackled in a future paper. The SSS simulated by ROM shows seasonal biases in the -1; +1 psu range, with a similar magnitude and spatial distribution than those in RCM4 (Sevault et al., 2014). The biases are higher in some problematic locations such as the northern Adriatic Sea and Dardanelles Strait (Fig. 9), a feature that also has been shown in previous studies (L'Hévéder et al., 2013; Di Luca et al., 2014; Sevault et al., 2014). The Mediterranean water fluxes simulated by ROM (Table 4) have been compared to available observations (Sanchez-Gomez et al., 2011; Soto-Navarro et al., 2014) and model (Sevault et al., 2014) estimates, providing a physically consistent assessment in the straits. ROM water balance terms over the Mediterranean Sea are similar to those obtained by

different authors (Table 4). The main difference is the exchange flows through the Strait of Gibraltar, where ROM presents estimates much lower than those presented by Soto-Navarro et al. (2014), although the net flow is in agreement with most of estimates.

The ROM SSH and surface (31m) circulation are able to reproduce the different quasi-permanent elevation/depression (anticyclonic/cyclonic) structures occurring in the Mediterranean Sea (Fig. 11). The cyclonic gyres (SSH depressions) correspond properly to the water mass formation sites. The 31m depth level has been chosen to remove the high-frequency variability of the uppermost ocean, while retaining a characteristic upper ocean circulation pattern. Also, the choice of this level depth makes our result more comparable with other works such as L'Hévéder et al. (2013) and Sevault et al. (2014). For 1980-2012 period the comparison between ROM and AVISO (SSALTO/DUACS, 2013) altimetry data (Fig. 12a) produced a quite satisfactory correlation of 0.61, close to the obtained by the RCSM4 (0.68). Finally, the ROM amplitude of the mean seasonal cycle measured was 12 cm while for AVISO was 14.5 cm and for RCSM4 16.9 cm (Fig. 12b). Thus, the model is able to satisfactorily reproduce the seasonal cycle and interannual variability of different oceanic variables.

The model also demonstrated good skills in reproducing the area-averaged interannual standard deviations of SST for the Mediterranean Sea (Fig. 16d). According to Fig. 16, ROM coupled system presents yearly SST standard deviations close to the reference OISST dataset. In fact, ROM does not only improve the yearly spatial standard deviations with respect to the MPI-ESMs (Figs. 16e and 16f) but also regarding to ERA-Interim and EN4 (Fig. 16b and 16c). The MPI-ESM-LR and -MR are not able to reproduce those local patterns due to the absence of resolution, thus indicating that the dynamical downscaling from MPI-ESM improves the simulation of GCMs.

In our simulations, the Mediterranean Sea will be warmer and saltier at the end of 21st century. Under the RCP8.5 scenario ROM provides integrated estimates of climate change similar to other models (Table 5). The mean Δ SST projected by ROM under RCP8.5 scenario is 2.73°C, close to MPI-ESM simulations, which show an SST increase of 2.80°C (-LR) and 2.87°C (-MR). It is also close to the mean increase (+2.6°C) projected by the CMIP5 ensemble of Shaltout and Omstedt (2014) (Table 5). The SST warming estimates under the RCP8.5 scenario agree with those obtained by Adloff et al. (2015) and with the multi-model Mediterranean of Darmakari et al. (2019), which show a mean increase of +3.1°C, with model increases ranging from +2.7 to +3.8°C. Despite differences horizontal resolutions, ROM expected warming (Fig. 13b) shows a similar spatial distribution to MPI-ESM-LR than MPI-ESM-MR (Figs. 14a and 14b). This is due to the ROM P1 simulation used to computed the Δ SST (ROM P1-ROM P2) was forced by MPI-ESM-LR. Figs. 15a and 15b shown how the warming that initially takes place at the surface layer is transported gradually to deeper layers. The warming expected by the models and its intensity will be strongly linked with the choice of emissions scenario.

As shown in Table 5, the mean Δ SSS projected by ROM under RCP8.5 is lower than those estimated by other authors (Somot et al., 2006; 2008, Adloff et al., 2015). This seems to be related to the fact that the SSS filed in the ROM RCP8.5 projection shows a dipolar structure in the Mediterranean (Fig. 13d). So far, previous works (Somot et al., 2006, Adloff et al., 2015) denoted positive values of Δ SSS over the whole Mediterranean Sea by the end of the century, which differ to our results. The ROM SSS decrease in the western basin could be related to the influence of surface waters from the Northeast

Eliminado: while Thorpe and Bigg (2000) using high resolution models under 2XCO₂ scenario is estimated a 4°C warming for the SST (Table 4). Somot et al., (2006) carried out a similar study using high resolution models forced by the SRES scenario A2. The results of their study are similar to those obtained in the present work. Later, Somot et al., (2008) used a RAOCM for the Mediterranean basin, to simulate the SRES A2 scenario during 1960-2099, obtaining a Δ SST of 2.6°C. ...

Eliminado: In MPI-ESM simulations for RCP 8.5 the SST shows an increase of 2.80°C (-LR) and 2.87°C (-MR).

Eliminado: All SST warming estimates are quite coherent with those obtained by Adloff et al., (2015) for different climate scenarios.

Atlantic. As we exposed in section 3.5, the MPI-ESM-LR and -MR models under RCP8.5 scenario also represent this dipolar pattern and the averaged increment of SSS shown by ROM into the Mediterranean Sea.

5 Conclusions

5 In this study, the regional atmosphere-ocean coupled model ROM (Sein et al., 2015) was described and validated for the Mediterranean region. The experiment in which our model is driven by ERA-Interim shows a good performance in simulating the present climate. ROM is able to reproduce the main characteristics of the Mediterranean Sea, providing a physically consistent estimation of the average behavior, seasonal cycle and interannual variability of both atmospheric and oceanic parameters.

10 The model also demonstrated improvements of local processes such as the exchange of water through the Gibraltar and Dardanelles Straits or internal seas behaviors contrasted to ESMs. The dynamical downscaling from MPI-ESM implemented in our AORCM offers high spatial resolutions, being capable of reproducing with a remarkable detail the main local and mesoscale processes that take place into the Mediterranean basin.

15 Our analysis of the simulations driven by the MPI-ESM RCP8.5 scenarios shows that by the end of the 21st century the Mediterranean Sea will be warmer and saltier across most of the basin. The temperature in the upper ocean layer during 2070-2099 period will increase in 2.73°C in comparison with the 1976-2005 control period, while the mean salinity will increase by 0.17 psu. The warming, that initially takes place at the surface propagates gradually to the deeper layers. Furthermore, it is very remarkable that the Western Mediterranean surface layer presents a salinity decreasing tendency, opposite to the rest of the Mediterranean.

20 Finally, we conclude that the ROM is a powerful model system that can be used to estimate possible impacts of climate change on regional scale. In the future, we plan to use our ROM coupled system to characterizing and analyzing the climate variability of deep water formations in the Mediterranean Sea.

Acknowledgements

25 Simulations were done at the German Climate Computing Centre (DKRZ). DS was supported by PRIMAVERA funding received from the European Commission under Grant Agreement 641727 of the Horizon 2020 research program and by the state assignment of FASO Russia (theme No. 0149-2019-0015).

References

- Adloff, F., Somot, S., Sevault, F., Jordà, G., Aznar, R., Déqué, M., Herrmann, M., Marcos, M., Dubois, C., Padorno, E. and Alvarez-Fanjul, E.: Mediterranean Sea response to climate change in an ensemble of twenty first century scenarios, *Clim. Dynam.*, 45 (9-10), 2775-2802, doi: 10.1007/s00382-015-2507-3, 2015.
- 5 [Akthar, N., Brauch, J., and Ahrens, B.: Climate modeling over the Mediterranean Sea: impact of resolution and ocean coupling. *Clim. Dynam.*, 51\(3\), 933-948, doi: 10.1007/s00382-017-3570-8, 2018.](#)
- Arakawa, A. and Lamb, V. R.: Computational design of the basic dynamical processes of the UCLA general circulation model, *General Circulation of the Atmosphere*, 17, 173–265, 1977.
- Artale, V., Calmanti, S., Carillo, A., Dell'Aquila, A., Herrmann, M., Pisacane, G., Ruti, P. M., Sannino, G., Struglia, M. V.,
- 10 [Giorgi, F., Bi, X., Pal, J. S. and Rauscher, S.: An atmosphere–ocean regional climate model for the Mediterranean area: assessment of a present climate simulation, *Clim. Dynam.*, 35\(5\), 721-740, doi: 10.1007/s00382-009-0691-8, 2010.](#)
- Bergamasco, A and Malanotte-Rizzoli, P.: The circulation of the Mediterranean Sea: a historical review of experimental investigations, *Adv. Ocean. Limol.*, 1:1, 11-28, doi:10.1080/19475721.2010.491656, 2010.
- Beuviel, J., Sevault, F., Herrmann, M., Kontoyiannis, H., Ludwig, W., Rixen, M., Stanev, E., Béranger, K. and Somot, S.:
- 15 [Modeling the Mediterranean Sea interannual variability during 1961-2000: focus on the Eastern Mediterranean Transient, *J. Geophys. Res.*, 115, C08017, doi: 10.1029/2009JC005950, 2010.](#)
- [Cavicchia, L., Gualdi, S., Sanna, A. and Oddo, P.: The Regional Ocean-Atmosphere Coupled Model COSMP-NEMO MFS, *CMCC Res. Paper. RP0254*, 2015.](#)
- [Darmaraki, S., Somot, S., Sevault, F., Nabat, P., Cabos Narvaez, W. D., Cavicchia, L., Djurdjevic, V., Li, L., Sannino, G.](#)
- 20 [and Sein, D. V.: Future evolution of Marine Heatwaves in the Mediterranean Sea, *Clim. Dynam.*, doi: 10.1007/s00382-019-04661-z, 2019.](#)
- Dee, D. P., Uppala, S. M., Simmons, A. J., Berrisford, P., Poli, P., Kobayashi, S., Andrae, U., Balmaseda, M. A., Balsamo, G., Bauer, P., Bechtold, P., Beljaars, A. C. M., van den Berg, L., Bidlot, J., Bormann, N., Delsol, C., Dragani, R., Fuentes, M., Geer, A. J., Haimberger, L., Healy, S. B., Hersbach, H., Hólm, E. V., Isaksen, I., Kallber, P., Kohler, M., Matricardi,
- 25 [M., McNally, A. P., Monge-Sanz, B. M., Morcrett, J. J., Park, B. K., Peubey, C., de Rosnay, P., Tavolato, C., Thépaut, J.N. and Vitart, F.: The ERA-Interim reanalysis: configuration and performance of the data assimilation system, *Q. J. Roy. Meteor. Soc.*, 137, 553–597, doi: 10.1002/qj.828, 2011.](#)
- [Déqué, M., and Piedelievre, J. P.: Latest issue climate simulation over Europe, *Clim. Dynam.*, 11, 321–339, doi: 10.1007/BF00215735, 1995.](#)
- 30 [Di Luca, A., Flaounas, E., Drobinski, P. and Lebeauupin-Brossier, C.: The atmospheric component of the Mediterranean Sea water budget in a WRF multi-physics ensemble and observations, *Clim. Dynam.*, 43 \(9-10\), 2349-2375, doi: 0.1007/s00382-014-2058-z, 2014.](#)

Eliminado: Dell'Aquila, A., Calmanti, S., Ruti, P., Struglia, M. V., Pisacane, G., Carillo, A. and Sannino, G.: Effects of seasonal cycle fluctuations in an AIB scenario over the Euro-Mediterranean region, *Clim. Res.*, 52, 135-157, doi: 10.3354/cr01037, 2012.

- Dubois, C., Somot, S., Calmanti, S., Carillo, A., Déqué, M., Dell'Aquila, A., Elizalde, A., Gualdi, S., Jacob, D., L'Hévéder, B., Li, L., Oddo, P., Sannino, G., Scoccimarro, E. and Sevault, F.: Future projections of the surface heat and water budgets of the Mediterranean Sea in an ensemble of coupled atmosphere–ocean regional climate models, *Clim. Dynam.*, 39 (7–8), 1859–1884, doi: 10.1007/s00382-011-1261-4, 2012.
- 5 [Fantini, A., Raffaele, F., Torma, C., Bacer, S., Coppola, E., Giorgi, F., Ahrens, B., Dubois, C., Sanchez, E. and Verdecchia, M.: Assessment of multiple daily precipitation statistics in ERA-Interim driven Med-CORDEX and EURO-CORDEX experiments against high resolution observations, *Clim. Dynam.*, 51 \(3\), 877-900, doi: 10.1007/s00382-016-3453-4, 2018.](#)
- Fratianni, C., Simoncelli, S., Pinardi, N., Cherchi, A., Grandi, A. and Dobricic, S.: Mediterranean RR 1955-2015 (Version1) [Dataset]. Copernicus Monitoring Environment Marine Service (CMEMS), doi: 10.25423/MEDSEA_REANALYSIS_PHY_006_009, 2015.
- 10 Giorgetta, M. A., Jungclaus, J., Reick, C. H., Legutke, S., Bader, J., Böttinger, M., Brovkin, V., Crueger, T., Esch, M., Fieg, K., Glushak, K., Gayler, V., Haak, H., Hollweg, H.-D., Ilyina, T., Kinne, S., Kornbluh, L., Matei, D., Mauritsen, T., Mikolajewicz, U., Mueller, W., Notz, D., Pithan, F., Raddatz, T., Rast, S., Redler, R., Roeckner, E., Schmidt, H., Schnur, R., Segschneider, J., Six, K. D., Stockhause, M., Timmreck, C., Wegner, J., Widmann, H., Wieners, K.-H., Claussen, M.,
- 15 Marotzke, J., Stevens, B.: Climate and carbon cycle changes from 1850 to 2100 in MPI-ESM simulations for the Coupled Model Intercomparison Project phase 5, *J. Adv. Model. Earth Sy.*, 5, 572–597, doi: 10.1002/jame.20038, 2013.
- [Giorgi, F. and Lionello, P.: Climate change projections for the Mediterranean region, *Global Planet. Change*, 63, 90–104, doi: 10.1016/j.gloplacha.2007.09.005, 2008.](#)
- Good, S. A., Martin, M. J. and Rayner, N. A.: EN4: Quality controlled ocean temperature and salinity profiles and monthly objective analyses with uncertainty estimates, *J. Geophys. Res.-Oceans.*, 118 (12), 6704-6716, doi: 10.1002/2013JC009067, 2013.
- Gouretski, V. and F. Reseghetti.: On depth and temperature biases in bathythermograph data: Development of a new correction scheme based on analysis of a global ocean database, *Deep-Sea Research I.*, 57, 812-833, doi:10.1016/j.dsr.2010.03.011, 2010.
- 25 Gualdi, S., Somot, S., Li, L., Artale, V., Adani, M., Bellucci, A., Braun, A., Calmanti, S., Carillo, A., Dell'Aquila, A., Déqué, M., Dubois, C., Elizalde, A., Harzallah, A., Jacob, D., L'Hévéder, B., May, W., Oddo, P., Ruti, P., Sanna, A., Sannino, G., Scoccimarro, E., Sevault, F. and Navarra, A.: The CIRCE simulations: regional climate change projections with realistic representation of the Mediterranean Sea, *B. Am. Meteorol. Soc.*, 94 (1), 65-81, doi: 10.1175/BAMS-D-11-00136.1, 2013.
- 30 Hagemann, S. and Dümenil-Gates, L.: A parameterization of the lateral waterflow for the global scale, *Clim. Dynam.*, 14, 17–31, doi: 10.1007/s003820050205, 1998.
- Hagemann, S. and Dümenil-Gates, L.: Validation of the hydrological cycle of ECMWF and NCEP reanalysis using the MPI hydrological discharge model, *J. Geophys. Res.* 106 (D2), 1503–1510, doi: 10.1029/2000JD900568, 2001.

- Hibler III, W.D.: A dynamic thermodynamic sea ice model, *J. Phys. Oceanogr.*, 9, 815–846, doi: 10.1175/1520-0485(1979)009<0815:ADTSIM>2.0.CO;2, 1979.
- Huffman, G., Bolvin, D., Braithwaite, D., Hsu, K., Joyce, R. and Xie, P.: Integrated Multi-satellite Retrievals for GPM (IMERG), version 4.4. NASA's Precipitation Processing Center, accessed 31 March, 2015, ftp://arthurhou.pps.eosdis.nasa.gov/gpmdata/, 2014.
- Ilyina, T., Six, K., Segschneider, J., Maier-Reimer, E., Li, H. and Nunez-Riboni, I.: Global ocean biogeochemistry model HAMOCC: Model architecture and performance as component of the MPI-Earth System Model in different CMIP5 experimental realizations, *J. Adv. Model. Earth Sy.*, doi: 10.1029/2012MS000178, 2013.
- IPCC.: Emissions Scenarios. Summary for Policymakers. A special Report of IPCC Working Group III, Cambridge University Press, Cambridge, 2000.
- IPCC.: Climate change 2013: the physical science basis. Working group I contribution to the fifth assessment report of the intergovernmental panel on climate change. Cambridge University Press, Cambridge, 2013.
- Jacob, D.: A note to the simulation of the annual and interannual variability of the water budget over the Baltic Sea drainage basin, *Meteorol. Atmos. Phys.*, 77(1-4), 61-73, doi: 10.1007/s007030170017, 2001.
- Jungclaus, J. H., Fischer, N., Haak, H., Lohmann, K., Marotzke, J., Matei, D., Mikolajewicz, U., Notz, D. and von Storch, J. S.: Characteristics of the ocean simulations in MPIOM, the ocean component of the MPI-Earth system model, *J. Adv. Model. Earth Sy.*, 5, 422–446, doi: 10.1002/jame.20023, 2013.
- L'Hévéder, B., Li, L., Sevault, F. and Somot, S.: Interannual variability of deep convection in the Northwestern Mediterranean simulated with a coupled AORCM, *Clim. Dynam.* 41 (3-4), 937-960, doi: 10.1007/s00382-012-1527-5, 2013.
- Li, H., Kanamitsu, M. and Hong, S. Y.: California reanalysis downscaling at 10 km using an ocean-atmosphere coupled regional model system, *J. Geophys. Res.*, 117, D12118, doi: 10.1029/2011JD017372, 2012.
- Macias, D., Garcia-Gorriz, E., Dosio, A., Stips, A. and Keuler, K.: Obtaining the correct sea surface temperature: bias correction of regional climate model data for the Mediterranean Sea, *Clim. Dynam.*, 51, 1095-1117, doi: 10.1007/s00382-016-3049-z, 2018.
- Maier-Reimer, E., Kriest, I., Segschneider, J. and Wetzel, P.: The Hamburg Ocean Carbon Cycle Model HAMOCC5.1 Technical Description Release 1.1, *Ber. Erdsystemforschung*, 14, http://hdl.handle.net/11858/00-001M-0000-0011-FF5C-D, 2005.
- Majewski, D.: The Europa-Modell of the Deutscher Wetterdienst. Seminar Proceedings ECMWF, Reading, vol. 2, 147–191, 1991.
- Marsland, S. J., Haak, H., Jungclaus, J. H., Latif, M. and Roeske, F.: The Max-Planck- Institute global ocean/sea ice model with orthogonal curvilinear coordinates, *Ocean Model.* 5 (2), 91–127, doi: 10.1016/S1463-5003(02)00015-X, 2003.

Eliminado: Herrmann, M., Somot, S., Calmanti, S., Dubois, C. and Sevault, F.: Representation of spatial and temporal variability of daily wind speed and of intense wind events over the Mediterranean Sea using dynamical downscaling: impact of the regional climate model configuration, *Nat. Hazards Earth Sys.*, 11, 1983-2001, doi: 10.5194/nhess-11-1983-2011, 2011.

Eliminado: Hourdin, F., Musat, I., Bony, S., Braconnot, P., Codron, F., Dufresne, J. L., Fairhead, L., Filiberti, M. A., Friedlingstein, P., Grandpeix J. Y., Krinner, G., LeVan, P., Li, Z. X. and Lott, F.: The LMDZ4 general circulation model: climate performance and sensitivity to parametrized physics with emphasis on tropical convection, *Clim. Dynam.*, 27 (7-8), 787-813, doi: 10.1007/s00382-006-0158-0, 2006.

- [Panthou, G., Vrac, M., Drobinski, P., Bastin, S. and Li, L.: Impact of model resolution and Mediterranean Sea coupling on hydrometeorological extremes in RCMs in the frame of HymMeX and MED-CORDEX, *Clim. Dynam.*, 51, 915-932, doi: 10.1007/s00382-016-3374-2, 2018.](#)
- Rechid, D. and Jacob, D.: Influence of monthly varying vegetation on the simulated climate in Europe, *Meteorol. Z.*, 15, 99–116, doi: 10.1127/0941-2948/2006/0091, 2006.
- Reick, C. H., Raddatz, T., Brovkin, V. and Gayler, V.: The representation of natural and anthropogenic land cover change in MPIESM, *J. Adv. Model. Earth Sy.*, 5, 1–24, doi: 10.1002/jame.20022, 2013.
- Reynolds, R. W., Smith, T. M., Liu, C., Chelton, D. B., Casey, K. S. and Schlax, M. G.: Daily High-Resolution-Blended Analyses for sea surface temperature, *J. Climate*, 20 (22), 5473-5496, doi: 10.1175/2007JCLI1824.1, 2007.
- 10 Roeckner, E., Arpe, K., Bengtsson, L., Christoph, M., Claussen, M., Dümenil, L., Esch, M., Giorgetta, M., Schlese, U. and Schulzweida, U.: The Atmospheric General Circulation Model ECHAM-4: Model description and simulation of present-day-climate, Rep. 218, MPI für Meteorol., Hamburg, Germany, 1996.
- Roeckner, E., Bäuml, G., Bonaventura, L., Brokopf, R., Esch, M., Giorgetta, M., Hagemann, S., Kirchner, I., Kornblüeh, L., Manzini, E., Schlese, U. and Schulzweida, U.: The atmospheric general circulation model ECHAM 5. PART I: Model description, Rep. 349, MPI für Meteorol., Hamburg, Germany, <http://hdl.handle.net/11858/00-001M-0000-0012-0144-5>, 2003.
- 15 Ruti, P. M., Somot, S., Giorgi, F., Dubois, C., Flaounas, E., Obermann, A., Dell'Aquila, A., Pisacane, G., Harzallah, A., Lombardi, E., Ahrens, B., Akhtar, N., Alias, A., Arsouze, T., Aznar, R., Bastin, S., Bartholy, J., Béranger, K., Beuvier, J., Bouffies-Cloch e, S., Brauch, J., Cabos, W., Calmanti, S., Calvet, J. C., Carrillo, A., Conte, D., Coppola, E., Djurdjevic, V., Dobrinski, P., Elizalde-Arellano, A., Gaertner, M., Galan, P., Gallardo, C., Gualdi, S., Goncalves, M., Jorba, O., Jorda, G., L'Heveder, B., Lebeaupin-Brossier, L., Li, L., Liguori, G., Lionello, P., Macias, D., Nabat, P.,  nol, B., Raikovic, B., Ramage, K., Sevault, F., Sannino, G., Struglia, M. V., Sanna, A., Tromba, C. and Vervatis, V.: MED-CORDEX initiative for Mediterranean Climate studies, *Bull. Am. Meteorol. Soc.*, 97 (7), 1187-1208, doi: 10.1175/BAMS-D-14-001761, 2015.
- S nchez-G mez, E., Somot, S., Josey, S. A., Dubois, C., Elguindi, N. and D qu e, M.: Evaluation of Mediterranean Sea water and heat budgets simulated by an ensemble of high resolution regional climate models, *Clim. Dynam.*, 37(9-10), 2067-2086, doi: 10.1007/s00382-011-1012-6, 2011.
- 25 [Sein, D. V., Koldunov, N. V., Pinto, J. G. and Cabos, W.: Sensitivity of simulated regional Arctic climate to the choice of coupled model domain. *Tellus A*, 66, 1-23966. doi: 10.3402/tellusa.v66.23966, 2014.](#)
- Sein, D. V., Mikolajewicz, U., Gr ger, M., Fast, I., Cabos, W., Pinto, J. G., Hagemann, S., Semmler, T., Izquierdo, A. and Jacob, D.: Regionally coupled atmosphere-ocean-sea ice-marine biogeochemistry model ROM: 1. Description and validation, *J. Adv. Model. Earth Sy.*, 7, 268–304, doi: 10.1002/2014MS000357, 2015.
- Sevault, F., Somot, S., Alias, A., Dubois, C., Lebeaupin-Brossier, C., Nabat, P., Adloff, F., D qu e, M. and Decharme, B.: A fully coupled Mediterranean regional climate system model: design and evaluation of the ocean component for the 1980–2012 period, *Tellus A*, 66, 1-23967, doi: 10.3402/tellusa.v66.23967, 2014.

Eliminado: Noilhan, J. and Mahfouf, J. F.: The ISBA land surface parameterization scheme, *Global Planet. Change*, 13 (1-4), 145-159, doi: 10.1016/0921-8181(95)00043-7, 1996.¶

Oki, T. and Sud, Y. C.: Design of total runoff integrating pathways (TRIP) - A Global River Channel Network, *Earth Interact.* 2, 1-36, doi: 10.1175/1087-3562(1998)002<0001:DOTRIP>2.3.CO;2, 1998.¶

Eliminado: Sannino, G., Hermann, M., Carrillo, A., Rupolo V., Ruggiero, V., Artale, V. and Heimbach, P.: An eddy-permitting model of the Mediterranean Sea with a two-way grid refinement at the Strait of Gibraltar, *Ocean Model.* 30, 56-72, doi: 10.1016/j.ocemod.2009.06.002, 2009.¶

- [Shaltout, M. and Omstedt, A.: Recent sea surface temperature trends and future scenarios for the Mediterranean Sea, *Oceanologia*, 56 \(3\), 411-443, doi: 10.5697/oc.56-3.411, 2014.](#)
- Simmons, A. J. and Burridge, D. M.: An energy and angular-momentum conserving vertical finite-difference scheme and hybrid vertical coordinate, *Mon. Weather. Rev.*, 109, 758–766, doi: 10.1175/1520-0493(1981)109<0758:AEAAMC>2.0.CO;2, 1981.
- 5 Somot, S., Sevault, F. and Déqué, M.: Transient climate change scenario simulation of the Mediterranean Sea for the 21st century using a high-resolution ocean circulation model, *Clim. Dynam.*, 27, 851–879, doi: 10.1007/s00382-006-0167-z, 2006.
- Somot, S., Sevault, F., Déqué, M. and Crépon, M.: 21st century climate change scenario for the Mediterranean using a coupled atmosphere–ocean regional climate model, *Global and Planet. Change*, 63 (2), 112-126, doi: 10.1016/j.gloplacha.2007.10.003, 2008.
- 10 [Somot, S., Ruti, P., Ahrens, B., Coppola, E., Jordà, G., Sannino, G. and Solmon, F.: Editorial for the Med-CORDEX special issue, *Clim. Dynam.*, 51, 771-777, doi: 10.1007/s00382-018-4325-x, 2018.](#)
- Soto-Navarro, J., Somot, S., Sevault, F., Beuvier, J., Criado-Aldeanueva, F., Garcia-Lafuente, J. and Béranger, K.: 15 Evaluation of regional ocean circulation models for the Mediterranean Sea at the Strait of Gibraltar: volume transport and thermohaline properties of the outflow, *Clim. Dynam.*, 44, 1277-1292, doi: 10.1007/s00382-014-2179-4, 2014.
- SSALTO/DUACS.: User Handbook (M)SLA and (M)ADT near-real time and delayed time products. Nomenclature: SALP-MU-P-EA-21065-CLS. Issue 3, Rev. 4. Reference: CLSDOS- NT-06-034, 2013.
- 20 Stevens, B., Giorgetta, M., Esch, M., Mauritsen, T., Crueger, T., Rast, S., Salzmann, M., Schmidt, H., Bader, J., Block, K., Brokopf, R., Fast, I., Kinne, S., Komblueh, L., Lohmann, U., Pincus, R., Reichler, R. and Roeckner, E.: Atmospheric component of the MPI-M Earth system model: ECHAM6, *J. Adv. Model. Earth Sy.*, 5, 146–172, doi: 10.1002/jame.20015, 2013.
- [Taylor, K., Stouffer, R. and Meehl, G.: An overview of CMIP5 and the experiments desing, *Bull. Am. Meteorol. Soc.*, 93 \(4\), 485-498, doi: 10.1175/BAMS-D-11-00094.1, 2012.](#)
- 25 Thorpe, R. B., and Bigg, G. R.: Modelling the sensitivity of the Mediterranean outflow to anthropogenically forced climate change, *Clim. Dynam.* 16, 355–368, doi: 10.1007/s003820050333, 2000.
- Tomczak, M. and Godfrey S. J.: *Regional Oceanography: an Introduction*, Pergamon, New York, 274-280, 1994.
- Valcke, S.: The OASIS3 coupler: a European climate modelling community software, *Geosci. Model Dev.*, 6, 373-388, doi: 10.5194/gmd-6-373-2013, 2013.

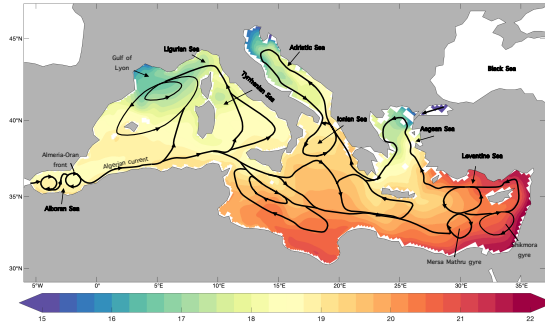


Figure 1: Mediterranean basin: 1980-2012 mean SST (°C) and upper ocean currents (Based on Tomczak and Godfrey, 1994).

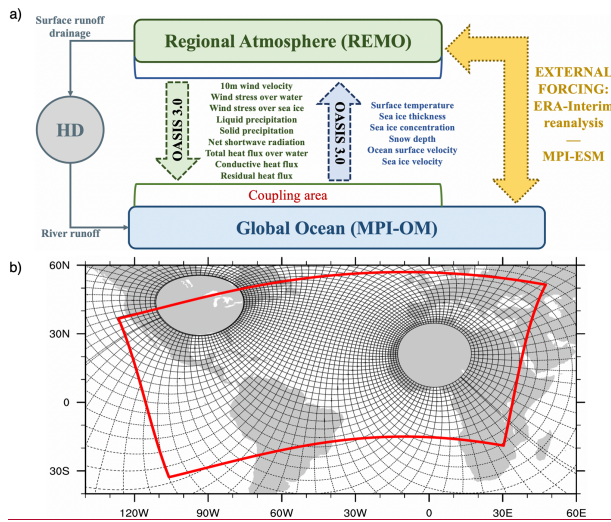
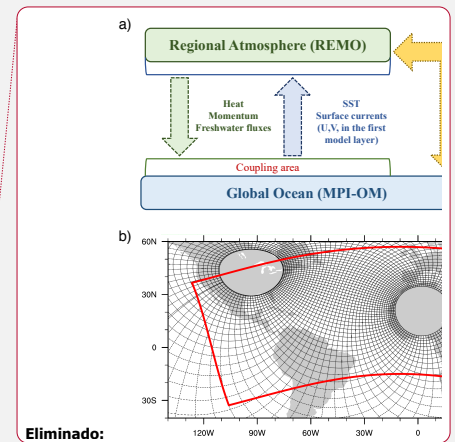


Figure 2: (a) ROM coupling scheme. (b) Atmospheric and oceanic ROM grids. MPI-OM variable resolution grid (black lines, drawn every twelfth), REMO domain (red line).



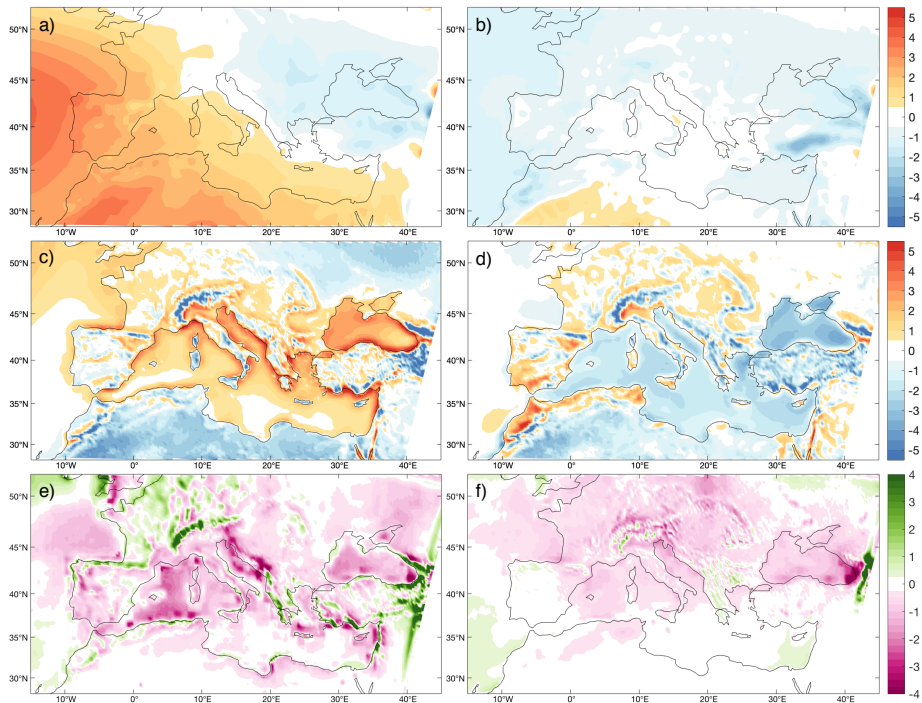


Figure 3: Differences ROM P0-ERA-Interim and TRMM for the 1980-2012 period in mean sea level pressure (MSLP, hPa) (upper row), near-surface (2m) temperature (T2m, °C) (middle) and precipitation (mm/d) (bottom). Left, DJF; right, JJA.

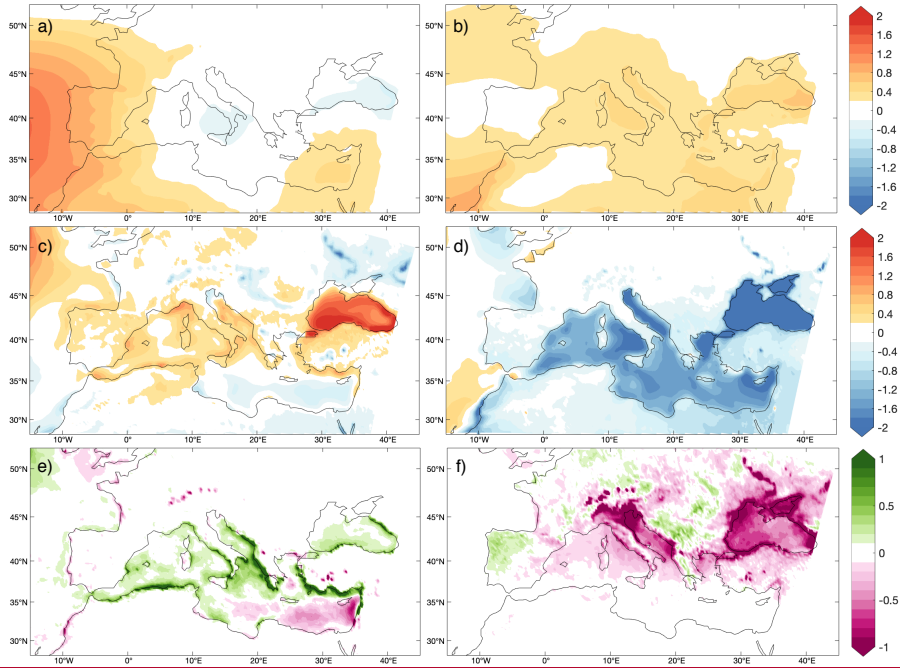


Figure 4: Differences ROM P0 and stand-alone REMO forced by ERA-Interim for the 1980-2012 period in mean sea level pressure (MSLP, hPa) (upper row), near-surface (2m) temperature (T2m, °C) (middle) and precipitation (mm/d) (bottom). Left, DJF; right, JJA.

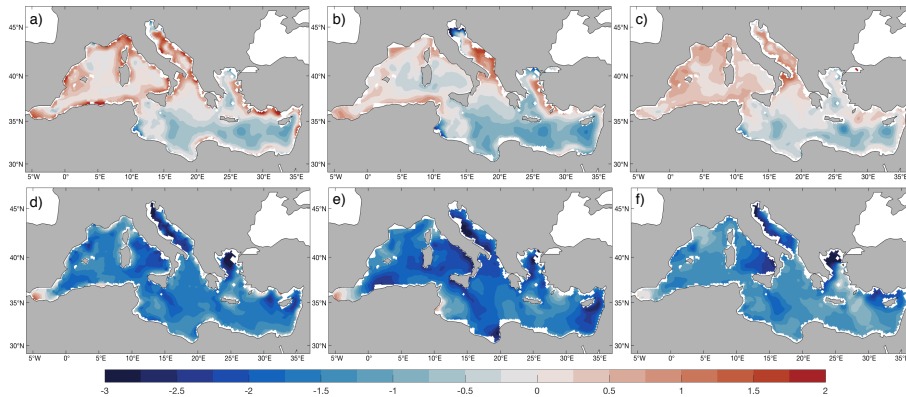
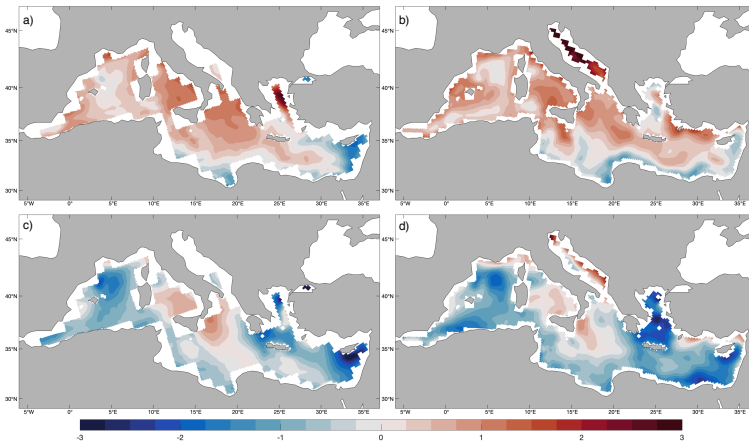


Figure 5: Difference between the ROM_P0 SST (°C) and the different climatologies (ERA-Interim [left], EN4 [middle] and OISST [right]) in winter (DJF, top), and summer (JJA, bottom).

Eliminado: 4



5 Figure 6: SST difference (°C) between ROM_P0 and MPI-ESM-LR (left) and -MR (right) in winter (DJF, top), and summer (JJA, bottom).

Eliminado: 5

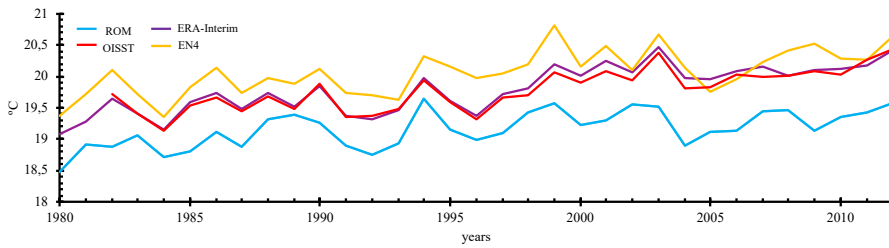
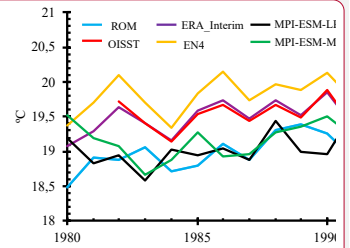


Figure 7: Time series of yearly mean (1980-2012) SST (°C) averaged over the Mediterranean basin. ROM P0 (blue), OISST (red), ERA-Interim (purple) and EN4 (yellow).



Eliminado:

Eliminado: 6

Eliminado: , MPI-ESM-LR (black) and MPI-ESM-MR (green).

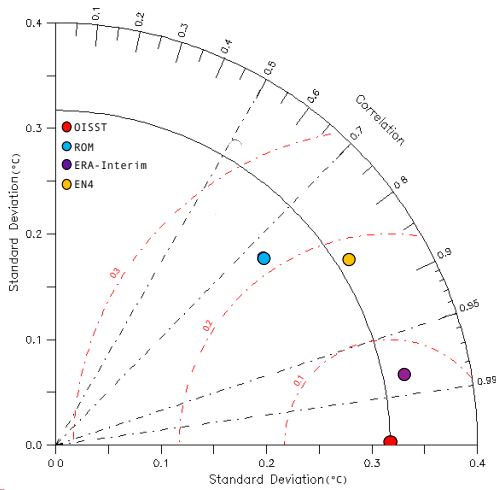
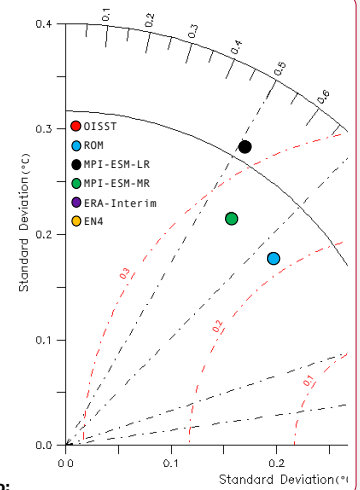


Figure 8: Taylor Diagram for Mediterranean SST during 1982-2012 period. The diagram summarizes the relationship between standard deviation (°C), correlation (r) and RMSE (red lines) (°C) for all data sets. The gridded OISST was employed as reference.



Eliminado:

Eliminado: 7

5

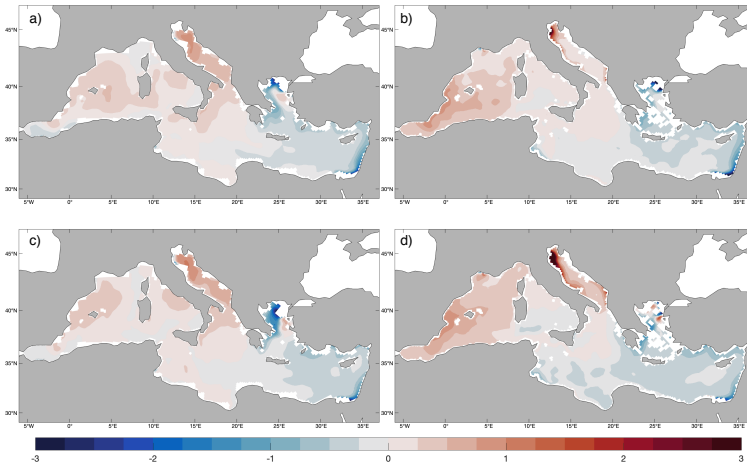
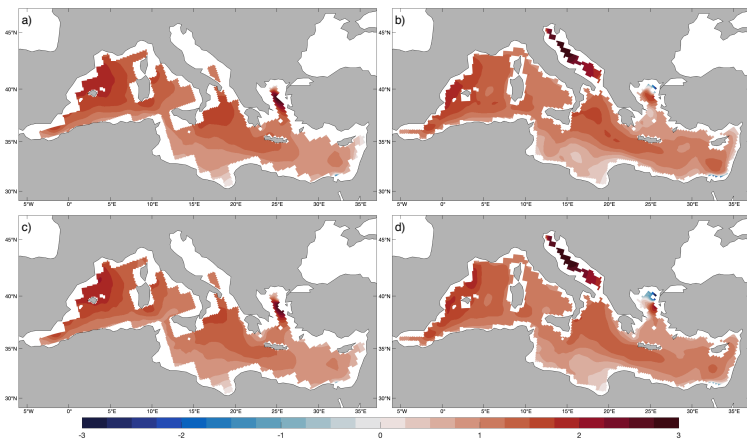


Figure 9: SSS (psu) difference between ROM_P0 the climatologies (EN4 [left] and CMEMS [right]) in winter (DJF, top), and summer (JJA, bottom).

Eliminado: 8



5 Figure 10: SSS (psu) difference between the ROM_P0 and MPI-ESM-LR (left), -MR (right) in winter (DJF, top), and summer (JJA, bottom).

Eliminado: 9

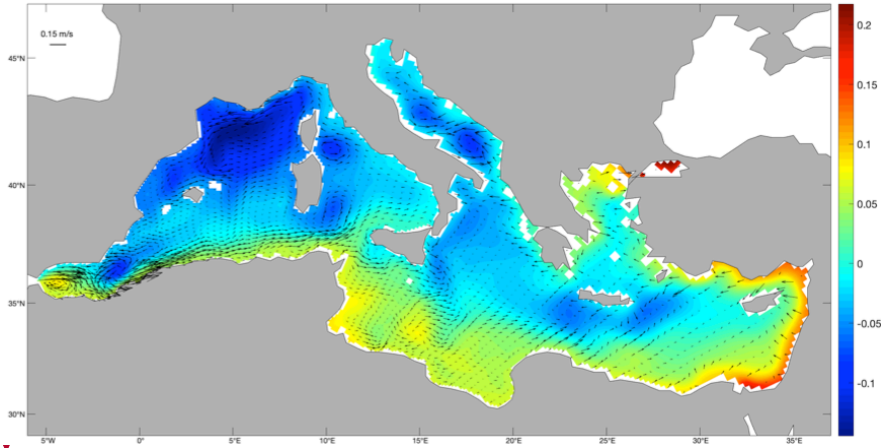
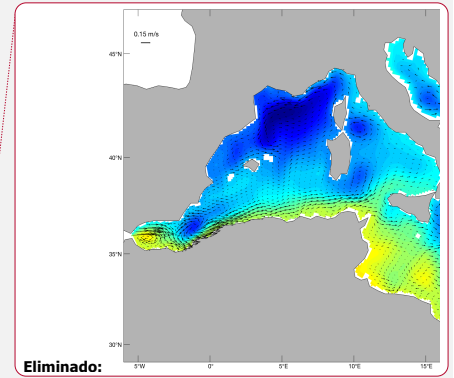
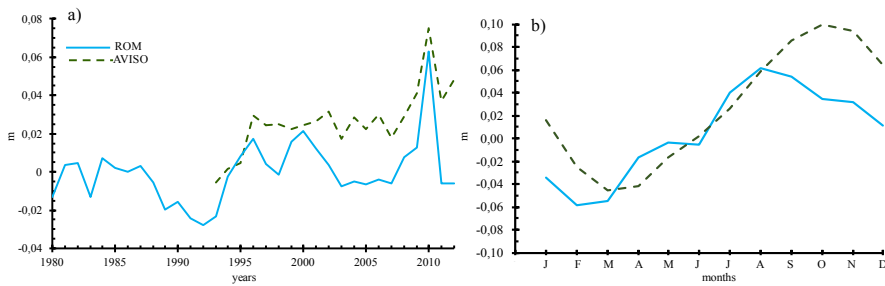


Figure 11: Mean (1980-2012) ROM_P0 SSH (m) and horizontal current velocity at 31 m depth (vectors, in m/s). Only every sixth vector is plotted.



Eliminado: 0



5 Figure 12: Time series of mean (1980-2012) sea-level anomalies averaged over the Mediterranean basin (left, in m). For ROM_P0 (blue), the dynamic SSH is added to the thermosteric term. Model data is compared to observations (AVISO, green dashed). ROM_P0 seasonal cycle is compared to AVISO data (right).

Eliminado: 1

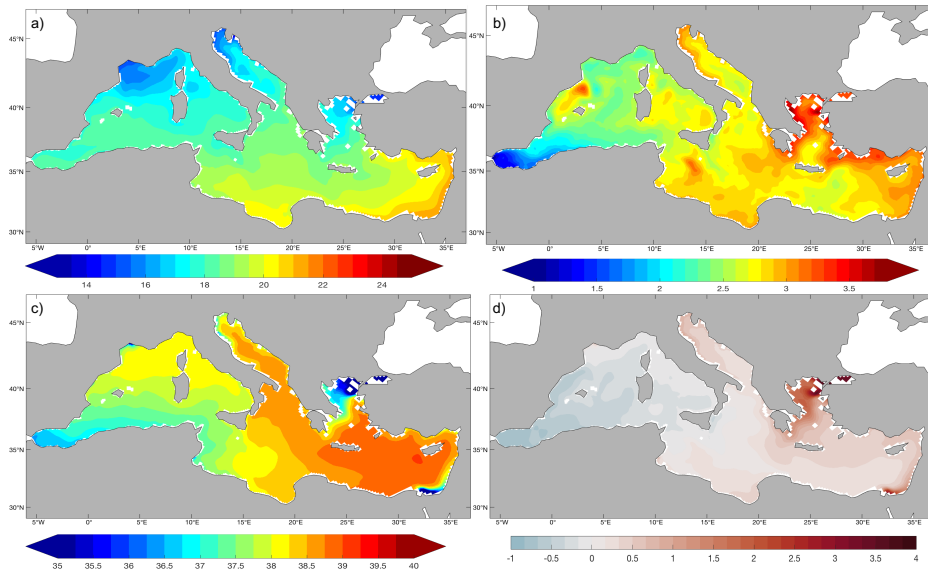


Figure 13: Mean SST (in °C, top left) and SSS (in psu, bottom left), averaged over the 1976-2005 period. Difference between mean SST (in °C, top right) and SSS (in psu, bottom right) RCP8.5 projection (2070-2099, ROM P2) and present climate (1976-2005, ROM P1).

Eliminado: 2

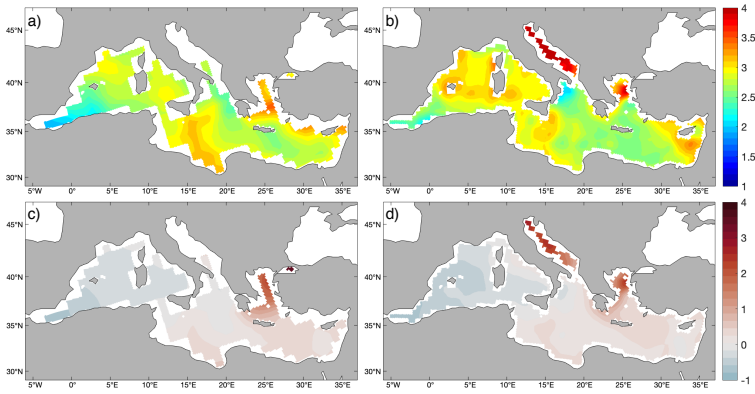


Figure 14: SST (in °C, upper row) and SSS (in psu, bottom) MPI-ESM-LR (left) and -MR (right) anomaly fields estimated as the difference between the averaged of the RCP8.5 projection (2070-2099) and present climate (1976-2005).

Eliminado: 3

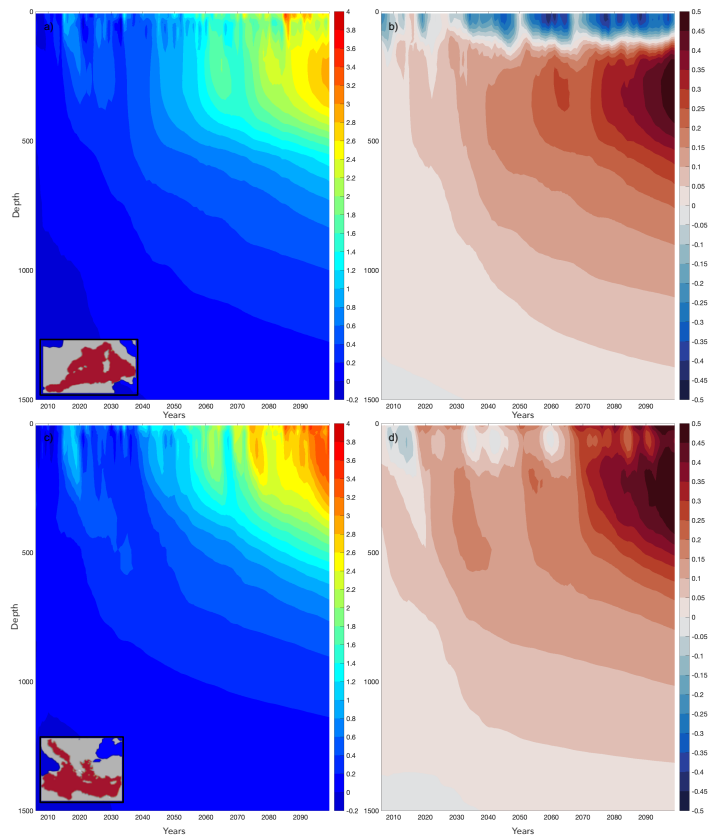


Figure 15: Temporal evolution of mean temperature (in °C, left) and salinity (in psu, right) along twenty-first century at Western (upper row) and Eastern Mediterranean (bottom).

Eliminado: 4

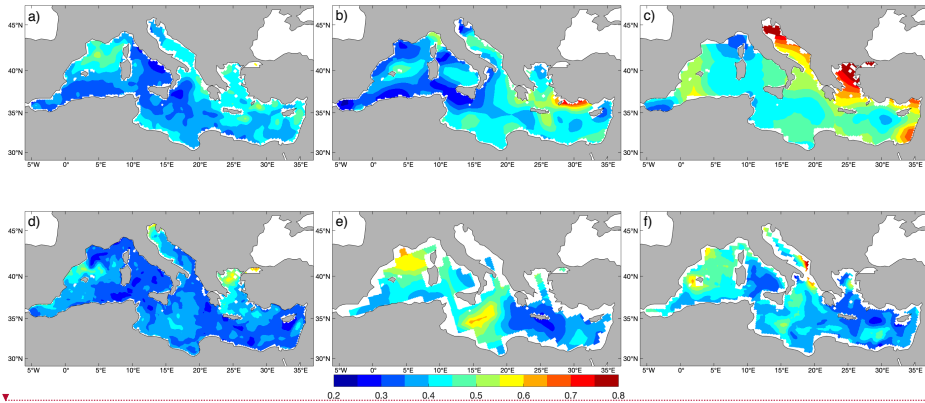
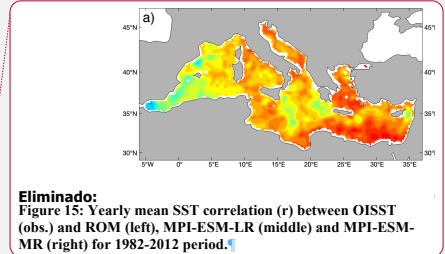


Figure 16: Yearly mean SST standard deviation (in °C) for 1982-2012 period: OISST (a), ERA-Interim (b), EN4 (c), ROM_P0 (d), MPI-ESM-LR (e) and MPI-ESM-MR (f).



Eliminado:
Figure 15: Yearly mean SST correlation (r) between OISST (obs.) and ROM (left), MPI-ESM-LR (middle) and MPI-ESM-MR (right) for 1982-2012 period.

Eliminado: 6

Table 1. Characteristics of ROM atmosphere-ocean regional coupled model used in this study. Modified from Darmaraki et al. (2019). For details see Scin et al. (2015).

<u>Institute</u>	<u>AWI/GERICS</u>
<u>Driving GCM</u>	<u>MPI-ESM-LR</u>
<u>Med. Sea Model</u>	<u>MPI-OM</u>
<u>Ocean Res.</u>	<u>7-25 km</u>
<u>Num. of z-levels (ocean)</u>	<u>40</u>
<u>SST (1st layer depth)</u>	<u>16 m</u>
<u>Timestep (ocean)</u>	<u>900 s</u>
<u>Atmosphere model</u>	<u>REMO</u>
<u>Atmosphere Res.</u>	<u>25 km</u>
<u>Coupling frequency</u>	<u>60 min</u>

Table 2. Datasets used in the ROM validation.

	Parameters	Period	Spatial resolution	Datasets
Atmosphere	MSLP	1980-2012	80 km (T255 spectral)	ERA-Interim (Dee et al., 2011)
	T2m	1980-2012	80 km (T255 spectral)	ERA-Interim (Dee et al., 2011)
	Precipitation	1997-2012	1/4° x 1/4°	TRMM (Huffman et al., 2014)
Ocean	SST	1982-2012	1/4° x 1/4°	OISST (Reynolds et al., 2007)
		1980-2012	80 km (T255 spectral)	ERA-Interim (Dee et al., 2011)
		1980-2012	1° x 1°	EN4 v.4.1.1 (Good et al., 2003; Gouretski and Reseghetti, 2010)
		1980-2012	1.5° x 1.5° / 0.4° x 0.4°	MPI-ESM-LR and -MR (Giorgetta et al., 2013)
	SSS	1980-2012	1° x 1°	EN4 v.4.1.1 (Good et al., 2003; Gouretski and Reseghetti, 2010)
		1980-2012	1/16° x 1/16°	CMEMS (Fратиanni et al., 2015)
		1980-2012	1.5° x 1.5° / 0.4° x 0.4°	MPI-ESM-LR and -MR (Giorgetta et al., 2013)
	SSH	1993-2012	1/4° x 1/4°	SSALTO/DUACS L4

Eliminado: 1

Table 3. Trend computed from yearly means during 1980-2012 by the different analysis into the Mediterranean Sea.

	<u>ROM P0</u>	<u>OISST</u>	<u>ERA Interim</u>	<u>EN4</u>	<u>MPI-ESM-LR</u>	<u>MPI-ESM-MR</u>
°C/year	+0.016	+0.027	+0.029	+0.022	+0.028	+0.020

Eliminado: 2

Table 4. Water balance and exchange flows for the Mediterranean Sea according to ROM_P0, RCSM4 and observation-based estimates. All results are presented in Sverdrups (Sv).

Eliminado: 3

Parameters	1980-2012 mean ROM_P0	RCSM4 Sevault et al., (2014)	Estimates
Evaporation	0.093	0.110	0.086-0.089 (Sánchez-Gómez et al., 2011)
Precipitation	0.034	0.040	0.020-0.047 (ibid)
Runoff	0.025	0.010	-
E-P	0.059	0.070	0.039-0.069 (ibid)
E-(P+R)	0.034	0.060	-
Gibraltar in	0.554	0.850	0.81 (Soto-Navarro et al., 2014)
Gibraltar out	0.524	0.800	0.78 (ibid)
Gibraltar net	0.030	0.050	0.04-0.10 (ibid)
Dardanelles in	0.132	-	-
Dardanelles out	0.109	-	-
Dardanelles net	0.023	0.007	0.008-0.01 (Sánchez-Gómez et al., 2011)

Table 5. Mediterranean Sea spatial averaged changes in SST and SSS at the end of the twenty-first century as compared with the present climate.

Eliminado: 4

	Scenario	Δ SST (°C)	Δ SSS (psu)
ROM	RCP8.5	+2.73	+0.17
MPI-ESM-LR	RCP8.5	+2.80	+0.10
MPI-ESM-MR	RCP8.5	+2.87	+0.12
Thorpe and Bigg (2000)	2XCO ₂	+4	-
Somot et al. (2006)	A2	+2.50	+0.33
Somot et al. (2008)	A2	+2.60	+0.43
<u>Shaltout and Omstedt (2014)</u>	<u>RCP2.6</u>	<u>+0.5</u>	<u>-</u>
<u>(ibid)</u>	<u>RCP4.5</u>	<u>+1.15</u>	<u>-</u>
<u>(ibid)</u>	<u>RCP6.0</u>	<u>+1.42</u>	<u>-</u>
<u>(ibid)</u>	<u>RCP8.5</u>	<u>+2.6</u>	<u>-</u>
<u>Adloff et al. (2015)</u>	<u>A2</u>	<u>+2.53</u>	<u>+0.48</u>
<u>(ibid)</u>	<u>A2-F</u>	<u>+2.97</u>	<u>+0.69</u>
<u>(ibid)</u>	<u>A2-ARF</u>	<u>+2.97</u>	<u>+0.89</u>
<u>(ibid)</u>	<u>B1-ARF</u>	<u>+1.73</u>	<u>+0.70</u>
<u>Darmaraki et al. (2019)</u>	<u>RCP8.5</u>	<u>+3.1</u>	<u>-</u>